IOPscience iopscience.iop.org

Home Search Collections Journals About Contact us My IOPscience

Morphology and magnetic behaviour of an Fe_3O_4 nanotube array

This content has been downloaded from IOPscience. Please scroll down to see the full text.

2006 J. Phys.: Condens. Matter 18 10545

(http://iopscience.iop.org/0953-8984/18/47/002)

View the table of contents for this issue, or go to the journal homepage for more

Download details:

IP Address: 207.162.240.147
This content was downloaded on 10/07/2017 at 02:13

Please note that terms and conditions apply.

You may also be interested in:

Synthesis, characterization and magnetic properties of Fe nanotubes
Y Xu, D S Xue, J L Fu et al.

Magnetic texture in iron nanowire arrays
J B Wang, X Z Zhou, Q F Liu et al.

The fabrication and magnetic properties of nanowire-like iron oxide
L Y Zhang, D S Xue, X F Xu et al.

Structure and magnetic study of Fe1-xNix
Jian-Bo Wang, Qing-Fang Liu, De-Sheng Xue et al.

Metal nanotubes prepared by a sol–gel method followed by a hydrogen reductionprocedure
Zhenghe Hua, Shaoguang Yang, Hongbo Huang et al.

Novel solid-state synthesis of alpha-Fe and Fe3O4 nanoparticles embedded in a MgOmatrix
O Schneeweiss, R Zboril, N Pizurova et al.

Influence of crystal orientation on magnetic properties of hcp Co nanowire arrays
Xianghua Han, Qingfang Liu, Jianbo Wang et al.

Magnetic moment orientations in nanowire arrays embedded in anodic aluminumoxide templates
Fashen Li, Liyuan Ren, Ziping Niu et al.

Microstructure and magnetic anisotropy of electrospun Cu1xZnxFe2O4 nanofibres: a local probe study
Zhiwei Li, Weiwei Pan, Junli Zhang et al.

INSTITUTE OF PHYSICS PUBLISHING JOURNAL OF PHYSICS: CONDENSED MATTER

J. Phys.: Condens. Matter **18** (2006) 10545–10551 doi:10.1088/0953-8984/18/47/002

Morphology and magnetic behaviour of an Fe_3O_4 nanotube array

Tao Wang[1], **Ying Wang, Fashen Li, Chongtao Xu and Dong Zhou**

Key Laboratory for Magnetism and Magnetic Materials of the Ministry of Education, Lanzhou University, Lanzhou 730000, People's Republic of China

E-mail: wangtlz@hotmail.com

Received 11 September 2006, in final form 12 October 2006
Published 8 November 2006
Online at stacks.iop.org/JPhysCM/18/10545

Abstract

An Fe_3O_4 nanotube array was successfully prepared in pores of an anodic aluminium oxide (AAO) template. Fe_3O_4 nanotubes and the nanotube array were characterized by transmission and scanning electron microscopy. The average diameter of the nanotubes was about 200 nm, and the length was more than 10 μm. The static distribution of the magnetic moments was investigated by means of magnetostatic energy analysis and Mössbauer spectrum measurement. The resulting Mössbauer spectrum shows that the distribution of the magnetic moments in the Fe_3O_4 nanotube array is spatially isotropic. However, macroscopic magnetic measurement shows the Fe_3O_4 nanotube array to have obvious anisotropy, and the easy axis is parallel to the nanotube axis. These magnetic behaviours are discussed on the basis of analysis of the magnetostatic energy.

1. Introduction

Magnetic nanostructures are a scientifically interesting and technologically important area of research with many present and future applications in biomedicine, magnetic recording, and spin electronics [1–3]. Researches on nanoparticles, nanowires, and ultrathin films have plenty of outcomes, and the search for novel geometries continues to be an important aspect of magnetic nanotechnology [4–6]. An emerging area is the synthesis of tubular nanostructures, which is pioneered in inorganic chemistry [7]. A few literature studies have reported the potential utilization of magnetic nanotubes in nanomedicine and biotechnological applications, nanoelectromechanical system devices, and nanotube-based multilayer nanostructures [7–11]. According to our knowledge, fabrication and research on magnetic properties of ferrite nanotube have few reports so far. Ferrite, especially Fe_3O_4, is an important material for various applications in industry and technology, for example spin electronics devices, magnetic

[1] Author to whom any correspondence should be addressed.

 © 2006 IOP Publishing Ltd Printed in the UK

fluids, and biosensors etc [12, 13]. Although Sui *et al* have fabricated a ferrite nanotube, the distribution of magnetic moments in the wall of the nanotube and the magnetic anisotropy were not investigated [14].

In this paper, we assembled an Fe_3O_4 nanotube array with high quality based on a porous anodic aluminium oxide (AAO) template prepared by ourselves in the lab. The static distribution of magnetic moments and the magnetic anisotropy were initially investigated by calculation of the demagnetization energy and analysis of the Mössbauer spectrum.

2. Experiment

The AAO template with pore diameter of about 200 nm was first prepared by anodic oxidation of 99.99% pure Al foil in phosphoric acid under a two-step anodizing process [15]. Then, the pores of as-prepared AAO template were loaded with 90 wt% $Fe(NO_3)_3 9{\cdot}H_2O$ solution. After that, the loaded template was cleaned and dried, and then heated to 350 °C for 3 h to decompose the iron nitrate. Finally, it was reduced at 300 °C in flowing hydrogen for 2 h to form an Fe_3O_4 nanotube array.

After the nanotube array was formed, it was etched in 0.1 M NaOH solution. The precipitates were dispersed in ethanol for TEM and SEM observation. The microscopic magnetic measurement was performed at room temperature by transmission Mössbauer spectroscopy with the γ-ray beam parallel to the nanotube axis. The γ-ray source of the Mössbauer spectrometer is 25 mCi ^{57}Co in Pd. Macroscopic magnetic properties were measured by a vibrating sample magnetometer (VSM) at room temperature.

3. Results and discussion

Figures 1(a) and (b) are TEM images of Fe_3O_4 nanotubes released from alumina. The average diameter is about 200 nm, and the length is more than 10 μm. It is clear from figure 1(b) that the wall of the Fe_3O_4 nanotube is compact and uniform. SEM images (figures 1(c) and (d)) of Fe_3O_4 nanotubes released from alumina further indicate that the nanotube wall is integrated. From the SAED pattern (figure 1(e)) of a single Fe_3O_4 nanotube it is obvious that the nantotube has a polycrystalline structure. The surface morphology of the nanotube array embedded in the AAO template was also characterized by SEM, as shown in figure 2. According to these images, each hole just hosts one nanotube, so that the morphology of the nanotube is defined by the internal shape of the hole and the overall density of the nanotube in the template is determined by the density of the holes. It is noticed that the diameter of nanotube and the inter-nanotube distance can be adjusted by controlling oxidation conditions of AAO template.

Figure 3 shows the XRD pattern of the Fe_3O_4 nanotube array. The reflection is characteristic of cubic spinel structure (space group $Fd3m$). Because maghemite (γ-Fe_2O_3) is easily formed due to oxidation during the formation of Fe_3O_4 and has almost the same XRD pattern as Fe_3O_4, it is difficult to distinguish Fe_3O_4 from γ-Fe_2O_3 by means of XRD. But the hyperfine parameters of Fe_3O_4 and γ-Fe_2O_3 are obviously different; for example the values of the magnetic hyperfine field at A and B sites of Fe_3O_4 are obviously different, while they are almost same in the case of γ-Fe_2O_3, so that Mössbauer spectroscopy is an effective method for distinguishing Fe_3O_4 from γ-Fe_2O_3. Figure 4 shows the collected Mössbauer spectrum of the sample at room temperature with the γ-ray parallel to the nanotube axis. The Mössbauer spectrum can be fitted with one doublet and three sextets. Sextets A and B correspond to the Fe ions of A and B sites of Fe_3O_4, respectively. The appearance of a small peak area of sextet C corresponding to α-Fe indicates that a small amount of α-Fe separated out during reduction process. From the peak area ratio, we estimated the concentration of α-Fe to be 5%. Because

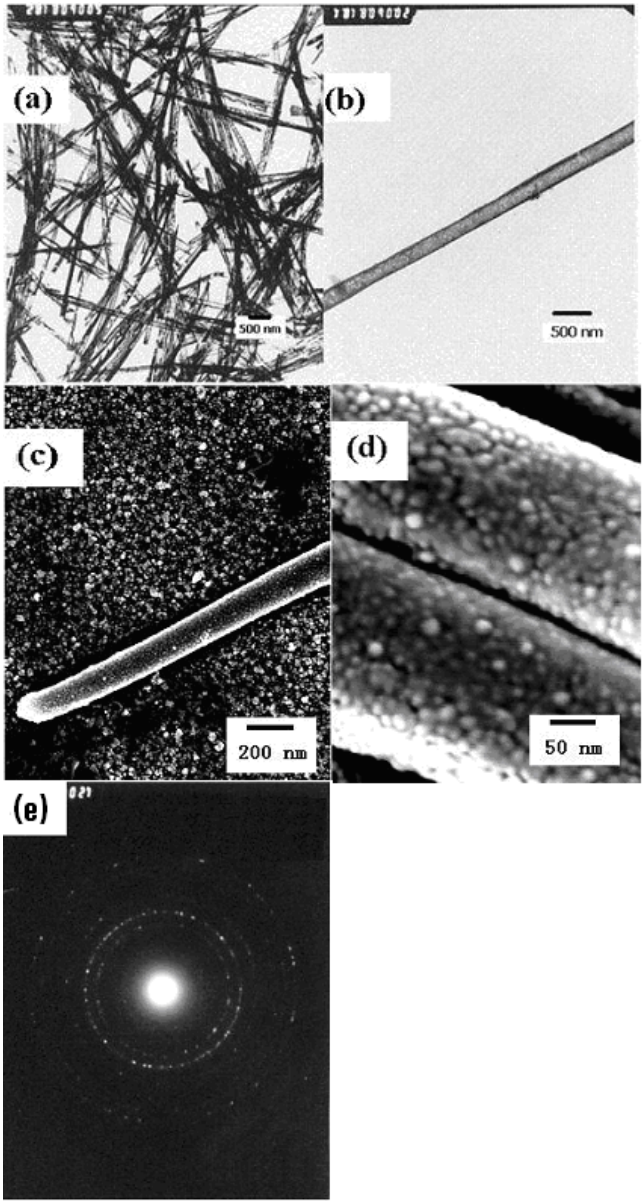

Figure 1. ((a) and (b)) TEM images of Fe_3O_4 nanotubes, ((c) and (d)) SEM image of an Fe_3O_4 nanotube, and (e) SAED pattern of a single Fe_3O_4 nanotube.

the Fe_2O_3 nanotube array has formed before the reduction process and the hydrogen can easily flow in the holes of nanotubes to reduce Fe_2O_3, we deduced the concentration of α-Fe to be uniform along the tube. The doublet D can be induced by two possible factors. One is spin disorder in the surface due to a large surface ratio; the other is the superparamagnetic phase resulting from the small particles in the polycrystalline nanotube array. In short, an Fe_3O_4 nanotube array with good morphology was successfully formed, although a small amount of α-Fe existed in the sample.

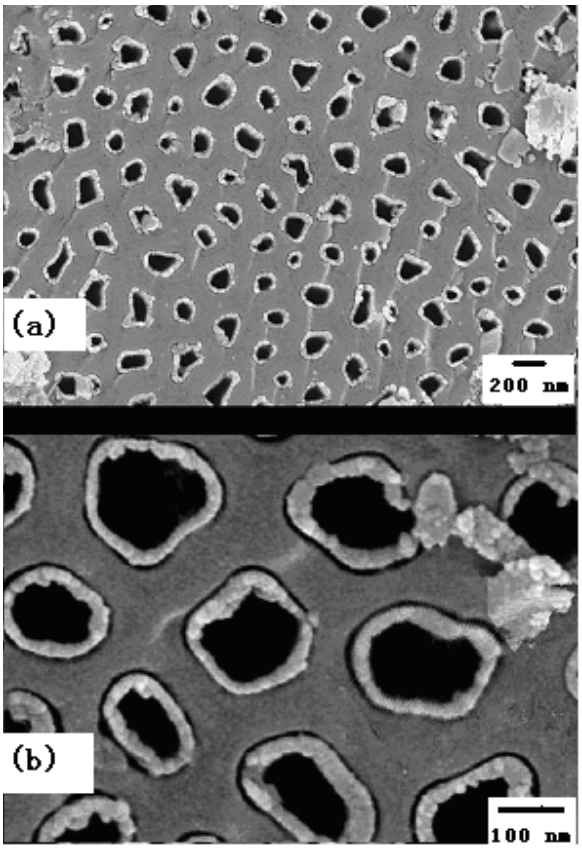

Figure 2. SEM images of an Fe_3O_4 nanotube array.

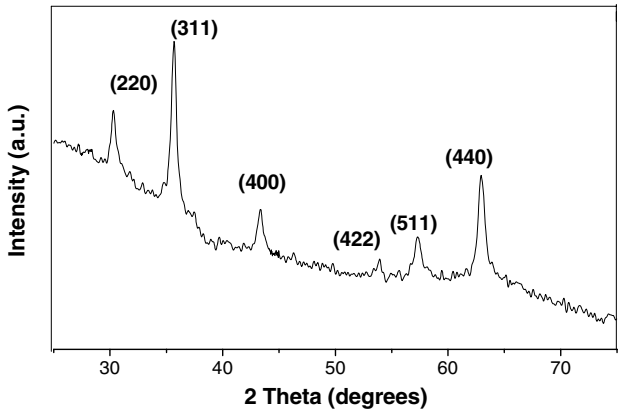

Figure 3. XRD pattern of the Fe_3O_4 nanotube array.

For one-dimensional magnetic nanowire, the demagnetization field tends to align the magnetic moments along the axis of the nanowire, which has been confirmed for Fe, FeCo alloy, and Fe oxide nanowire arrays by transmission Mössbauer spectroscopy [16]. For two-

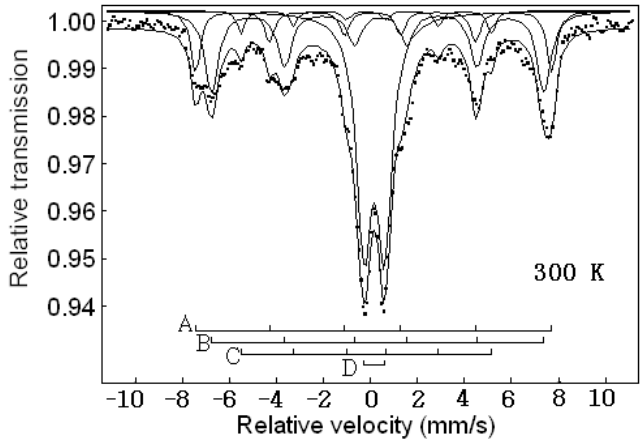

Figure 4. Mössbauer spectrum of the Fe_3O_4 nanotube array.

dimensional thin magnetic film, the demagnetization field tends to push down the magnetic moments in the plane. As a one-dimensional material, a nanotube has a more particular shape. Understanding of the static distribution of magnetic moments in nanotubes is the basis for further study of the magnetic behaviours. In order to study the static distribution of magnetic moments, we first calculate the demagnetization factor of the nanotube using the theory of magnetic charge. Figure 5(a) gives a nanotube scheme in which a three-dimensional orthogonal coordinate is set up in the centre of nanotube. As the aspect ratio is greater than 50, the demagnetization factor along the nanotube axis approximates to 0. We defined the value of the length as 10 000 nm for the calculation. The values of the outer and inner radius are 100 and 88 nm according to the result from TEM observation, and we suppose the nanotube to be magnetized to saturation under an external magnetic field along the Y axis. According to the theory of magnetic charge, demagnetization factors of various parts in the nanotube wall in the X–Y plane are shown in figure 5(b). β is the angle between the line connecting O and a random point in the nanotube wall and the Y axis. When β is 0 (point A in the nanotube wall), the demagnetization factor has the largest value of 0.94. With the increasing of β, it decreases to the smallest value of 0.06 at $\beta = 90^\circ$ (point B in the nanotube wall), and subsequently increases.

For a random part in the wall of the Fe_3O_4 nanotube, the final state originates from the minimization of the total energy density function:

$$E_{\text{total}} = E_{\text{exchange}} + E_{\text{K}} + E_{\text{demag}}, \tag{1}$$

where E_{exchange}, E_{K}, and E_{demag} are exchange, magnetocrystalline anisotropy, and demagnetization energies, respectively. Demagnetization energy tends to put the magnetic moments in the wall of the nanotube, and magnetocrystalline anisotropy energy tends to align the magnetic moments along the easy axis of grain. We assume that the magnetocrystalline anisotropy and saturation magnetization of the Fe_3O_4 nanotube are equal to those of bulk Fe_3O_4. The largest demagnetization energy E_{demag} in the nanotube wall is $0.94 \times 2\pi Ms^2 = 1.38 \times 10^6$ erg cm^{-3}, while the magnetocrystalline anisotropy energy E_{K} is only -1.35×10^5 erg cm^{-3}. Since the magnetocrystalline anisotropy energy is much smaller than the demagnetization energy, it can be ignored [17]. As a result, we deduce that the magnetic moments of Fe_3O_4 nanotube preferentially lie parallel to the nanotube wall for minimizing the magnetostatic energy.

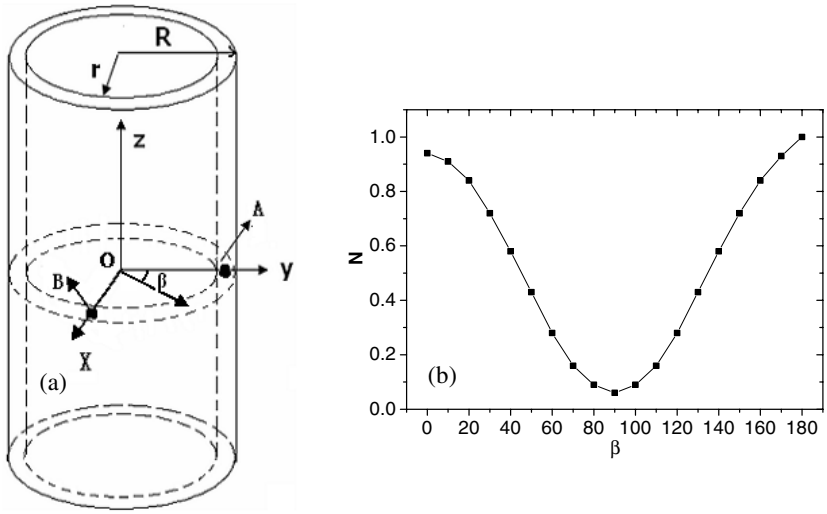

Figure 5. (a) Schematic illustration of a nanotube; (b) demagnetization factor depending on angle (β); β is the angle between the line connecting point O and a random point in the wall in the X–Y plane and the Y axis.

The distribution of magnetic moments can be investigated by transmission Mössbauer spectroscopy. In the Mössbauer spectrum, the intensity ratio of 2, 5 peaks and 1, 6 peaks ($I_{2,5}/I_{1,6}$) depends on the angle between the γ beam and magnetic moments in the sample, and can be written as

$$I_{2,5}/I_{1,6} = \frac{4\sin^2\theta}{3(1+\cos^2\theta)} = \frac{4(1-\cos^2\theta)}{3(1+\cos^2\theta)}. \tag{2}$$

When $\theta = 0$, the intensity ratio $I_{2,5}/I_{1,6}$ is 0, and $I_{2,5}/I_{1,6}$ is 4/3 when $\theta = 90°$. If the distribution of magnetic moments is spatially isotropic, $I_{2,5}/I_{1,6}$ is 2/3 [18]. From figure 4 $I_{2,5}/I_{1,6}$ is 0.64 for A and B sextets, which indicates that the distribution of magnetic moments in the nanotube array is spatially isotropic. Combining with the analysis of the magnetostatic energy, we conclude that the magnetic moments of the Fe_3O_4 nanotube preferentially lie in the nanotube wall, but the distribution is spatially isotropic. This can be understood from another explicit method: if an Fe_3O_4 tube is imagined to be unfolded to a thin film, the magnetic moments preferentially lie in the plane, but the distribution of magnetic moments in the plane is random. Perhaps there are domains existing in nanotube wall, which results in no magnetic texture.

Figure 6 shows the hysteresis loops of the Fe_3O_4 nanotube array with applied field parallel and perpendicular to the nanotube axis at room temperature. As the applied field is up to 1 T, the sample is still not saturated due to the possible spin disorder in the surface and superparamagnetic phase, which have been observed using Mössbauer spectroscopy. From the figure we can see that there are obvious differences between the two hysteresis loops. When the applied field is parallel to the nanotube axis, the sample can be magnetized more easily, and the coercivity and squareness ratio are larger than the values obtained when the applied field is perpendicular to the nanotube axis, so the Fe_3O_4 nanotube array has obvious magnetic anisotropy. The result for the hysteresis loops is consistent with the analysis of the magnetostatic energy. The demagnetization factor is near to 0 along the nanotube axis, but this not the case perpendicular to the axis (here it depends on β). As a result, when the sample

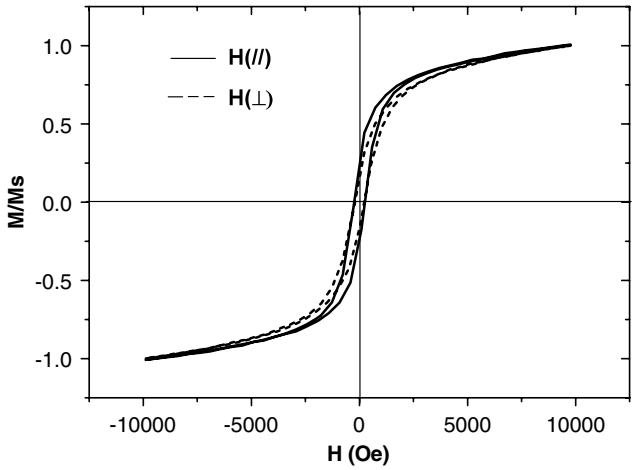

Figure 6. Magnetic hysteresis loops of the Fe_3O_4 nanotube array at room temperature with fields applied parallel (solid line) and perpendicular (dashed line) to the nanotube axis.

is measured with a perpendicular field, the sample is more difficult to magnetize than for measurement with a parallel field. In addition, the coercivities of the Fe_3O_4 nanotube array measured in parallel and perpendicular fields are 240 and 205 Oe, which are larger than the coercivity of bulk Fe_3O_4 (115–150 Oe) [17].

4. Conclusions

A high quality Fe_3O_4 array was successfully prepared in pores of anodic aluminium oxide (AAO) template. Through analysis of the magnetostatic energy and Mössbauer spectrum we conclude that the magnetic moments of the Fe_3O_4 nanotube array preferentially lie parallel to the nanotube wall, and the distribution of magnetic moments in the nanotube array is spatially isotropic. The Fe_3O_4 nanotube array exhibits obvious magnetic anisotropy, and the easy axis is parallel to the nanotube axis.

References

[1] Berry C C and Curtis A S D 2003 *J. Phys. D: Appl. Phys.* **46** R198
[2] Zhu J G 1993 *IEEE Trans. Magn.* **29** 195
[3] Žutić I and Fabian J 2004 *Rev. Mod. Phys.* **76** 323
[4] Sudakar C, Subbanna G N and Kutty T R N 2003 *J. Appl. Phys.* **94** 6030
[5] Fodor P S, Tsoi G M and Wenger L E 2003 *J. Appl. Phys.* **93** 7035
[6] Skomski R 2003 *J. Phys.: Condens. Matter* **15** R841
[7] Bao J C, Tie C Y, Xu Z, Zhou Q F, Shen D and Ma Q 2001 *Adv. Mater.* **13** 1631
[8] Gasparac R, Kohli P, Mota M O, Trofin L and Martin C R 2004 *Nano Lett.* **4** 513
[9] Son S J, Reichel J, He B, Schuchman S and Lee S B 2005 *J. Am. Chem. Soc.* **127** 7316
[10] Haberzettl C A 2002 *Nanotechnology* **13** R9
[11] Zahn M 2001 *J. Nanopart. Res.* **3** 73
[12] Nakamura T and Hankui E 2002 *J. Magn. Magn. Mater.* **257** 158
[13] Sui Y C, Skomski R, Sorge K D and Sellmyer D J 2004 *Appl. Phys. Lett.* **84** 1525
[14] Jeyadevan B, Chinnasamy C N, Shinoda K and Tohji K 2003 *J. Appl. Phys.* **93** 8450
[15] Li F S, Wang T, Ren L Y and Sun J R 2004 *J. Phys.: Condens. Matter* **16** 8053
[16] Li F S, Ren L Y, Niu Z P, Wang H X and Wang T 2002 *J. Phys.: Condens. Matter* **14** 6875
[17] Goya G F, Berquó T S and Fonseca F C 2003 *J. Appl. Phys.* **94** 3520
Preston R S, Hanna S S and Heberle J 1962 *Phys. Rev.* **128** 2207